# Plasma uniformity experiments using lens-shaped electrodes in a large area VHF reactor

H. Schmidt, L. Sansonnens, A. A. Howling,* and Ch. Hollenstein

*Centre de Recherches en Physique des Plasmas*

*Ecole Polytechnique Fédérale de Lausanne*

*PPH – Ecublens, CH-1015 Lausanne, Switzerland*

M. Elyaakoubi and J. P. M. Schmitt

*Unaxis Displays, 5 Rue Léon Blum, F-91120 Palaiseau, France*

(Dated: October 29, 2003)

## Abstract

Experiments using a lens-shaped circular electrode are described to measure the correction of plasma non-uniformity due to the standing wave effect in a large area Very High Frequency (VHF) plasma reactor. This work is the experimental verification of the theoretical reactor design in cylindrical geometry recently presented by L. Sansonnens and J. Schmitt *Appl. Phys. Lett.* **82** 182 (2003). It is found that the lens-shaped electrode effectively compensates the standing wave effects by creating a uniform RF vertical electric field in the plasma volume. The plasma is uniform, except for edge effects, for a wide range of parameters and consequently the design is suitable for plasma processing.

PACS numbers: 52.50.Dg, 52.80.Pi, 81.15.Gh

*Electronic address: `alan.howling@epfl.ch`

## I. INTRODUCTION

Capacitively-coupled parallel plate RF reactors are commonly used for plasma enhanced chemical vapor deposition (PECVD) and dry etching of thin films such as amorphous silicon or silicon oxide. Large area (> 1 $m^2$) reactors are used for the production of photovoltaic solar cells and thin film transistors for flat screens. These industrial applications typically require a uniformity in film thickness to better than $\pm 10\%$. There is also a strong interest in using frequencies higher than the industrial standard 13.56 MHz for PECVD [1] because of advantages such as high deposition rate [2], and reduced sheath voltage and ion bombardment energy [3]. However, when higher frequency is combined with large substrate size, standing wave effects cause problems of non-uniformity in conventional parallel plate reactors.

The non-uniformity considered in this paper is due to finite wavelength effects associated with high frequencies in large area reactors, such that the reactor size is larger than a tenth of the free space wavelength at the excitation frequency [4–9]. Non-uniform RF plasma potential will generally result in non-uniform power dissipation and consequently non-uniform deposition or etch rates.

Many other phenomena can also give rise to non-uniform deposition or etching in RF parallel plate reactors, including imperfect contact of the substrate with the electrode [10], inappropriate gas flow distribution [9], clouds of dust particles [11], and various edge effects due to electrostatic fringing and electromagnetic fields [7] and electrode asymmetry [12, 13]. Depending on the plasma parameters and reactor design, these effects can be significant also at low excitation frequencies (13.56 MHz) in parallel plate reactors, and will remain even if the standing wave effects can be eliminated for VHF operation (Very High Frequency: 30 MHz to 300 MHz; vacuum wavelength 10 m to 1 m).

This paper is organized as follows: Section II describes the Gaussian-lens electrode, the reactor and diagnostics. Section III presents the measurements of the electric field in vacuum, and the results for the plasma uniformity with parallel plate electrodes and with the Gaussian-lens electrode.

## II. EXPERIMENTAL ARRANGEMENT

A schematic of the 1 m-diameter cylindrical reactor is shown in figure 1; a cylindrical reactor was used to facilitate comparison with the 2D cylindrical $(r, z)$ vacuum theory in reference [8]. Moreover, cylindrical symmetry means that a single line of probes across

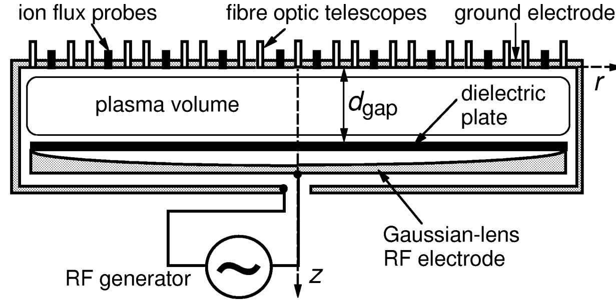


FIG. 1: Schematic of the cylindrical, capacitively-coupled RF reactor. Electrode radius 0.5 m, grounded sidewall radius 0.51 m, electrode gap 0.03 m. For the Gaussian-lens experiments, the dielectric plate was a glass disc; for parallel plate experiments, the glass was replaced by a metal disc to form a plane RF electrode. 19 fibre optic telescopes and 10 electrostatic probes are mounted along a diameter in the surface of the ground electrode.

a radius should suffice to characterize the plasma uniformity, in contrast to a rectangular reactor where a 2D array is necessary. In these experiments, measurements were made across a whole diameter to check the cylindrical symmetry. The lens design of the RF electrode is intended to compensate the standing wave effect by creating a uniform vertical electric field over the plasma volume. To be uniform, the plasma requires not only a constant electric field, but also a constant geometrical thickness. The plasma was therefore confined between parallel boundaries by a dielectric plate - a glass disc in these experiments - placed on the profiled electrode (see figure 1) [8]. The RF voltage between this dielectric sheet and the flat ground electrode would therefore be uniform in presence of a uniform electric field.

A special RF electrode was designed whose surface was machined according to a Gaussian profile [8]:

$$z = a_0 \exp(-k_0^2 r^2/4) \tag{1}$$

where $k_0$ is the vacuum wavenumber for the chosen excitation frequency and $a_0$ corresponds

to the total electrode gap on axis. The plasma gap height (including sheaths) is therefore

$$d_{\mathrm{gap}} = a_0 \exp(-k_0^2 R^2/4) \tag{2}$$

where $R$ is the reactor radius. In this work, $R = 50$ cm, $d_{\mathrm{gap}} = 3$ cm, $a_0 = 3.9$ cm, and the lens thickness on axis, $a_0 - d_{\mathrm{gap}} = 0.9$ cm. The Gaussian profile is a good approximation to the exact profile given in Ref. [8] provided that $k_0 a_0 \ll 1$ which is satisfied here. The design frequency $f_0$ is $ck_0/2\pi$ where $c$ is the speed of light in vacuum. The electrode was constructed for uniform electric field at a design frequency of 100 MHz. Conventional parallel-plate electrodes were also used for comparison, by replacing the glass with a metal disc.

A dielectric convex "lens" can be used to fill the gap below the dielectric plate to prevent any possible ignition of a parasitic plasma there, in which case the wavenumber becomes $k_0\sqrt{\epsilon_{\mathrm{r}}}$ [8] and the design frequency is reduced by a factor $\sqrt{\epsilon_{\mathrm{r}}}$. The dielectric used in this work was PTFE (relative dielectric constant $\epsilon_{\mathrm{r}} = 2.1$) and so the modified design frequency of the lens filled with PTFE was $100/\sqrt{2.1} = 69.0$ MHz.

All experiments were performed at room temperature using argon gas. The pressure range was 5 to 750 mTorr with RF power from 50 to 300 W. Three RF generators with frequencies 13.56, 67.8 and 100 MHz were used. The RF generators were capacitively-coupled to the reactor axis via an impedance matching network and stripline. The RF power was measured with a voltage, current and phase wideband probe placed after the impedance matching network.

The radial profile of the RF vertical electric field strength in vacuum was measured by drawing a calibrated diode probe [14] across the reactor diameter at mid-gap height through a small window in the reactor sidewall.

The plasma uniformity was monitored by means of two probe arrays positioned along the same diameter. Nineteen fiber optic telescope probes with photodiode sensors, calibrated *in situ*, measured the optical emission intensity averaged over the vertical profile to give a rough indication of the plasma power radial profile [15]. The upper surface of the glass had a matt black coating to minimize stray reflections into the fiber optic telescope probes. Ten surface mounted biased (-50 V) electrostatic probes measured the ion Bohm current through the sheath to give an estimation of the ion flux onto the plane ground electrode.

## III. RESULTS AND DISCUSSION

### A. Electric field measurements in vacuum

The radial profile of the vertical electric field strength $E_z(r)$ without plasma was measured for three frequencies as shown in figure 2 for parallel plates and for the Gaussian-lens electrode designed for 100 MHz operation (without the PTFE dielectric filling).

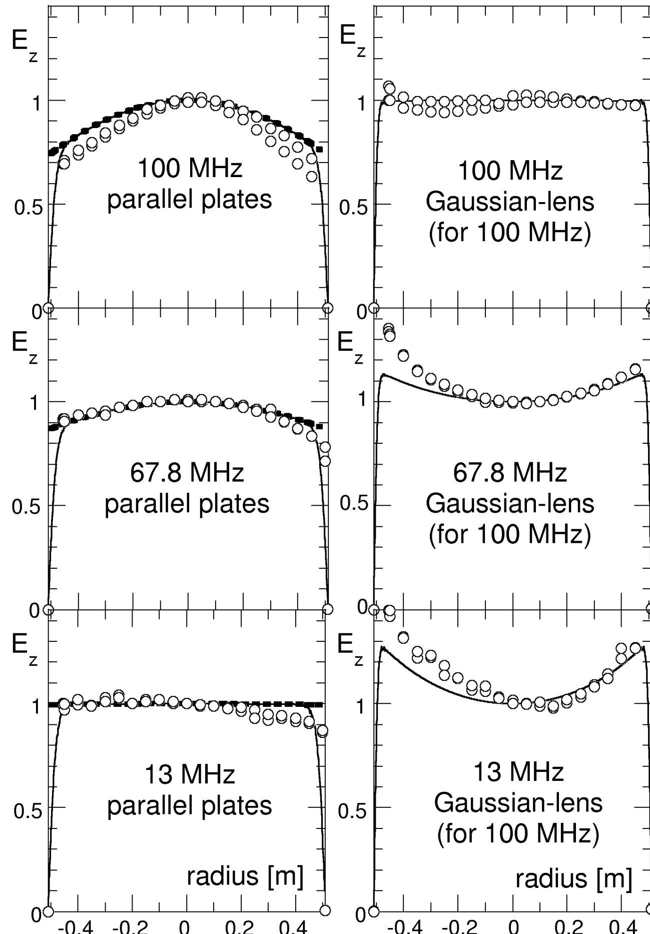


FIG. 2: Measured and modeled radial profiles of the vertical electric field in vacuum for frequencies 13.56, 67.8 and 100 MHz. Left-hand column: with parallel plate electrodes. Right-hand column: using the Gaussian vacuum lens electrode (design frequency 100 MHz). The data points are compared with numerical solutions of Maxwell's equations (continuous line) for the corresponding electrode geometry, and also with Bessel functions (dotted line) for the parallel plate case. Error bars of $\pm 7\%$ are omitted for clarity. All data are normalised to the values on axis.

Solution of Maxwell's equations with parallel electrodes [8] gives a Bessel function profile

$$E_z(r) = E_0 \mathrm{J}_0 \left[ k_0 r \right] \tag{3}$$

where $k_0$ is the vacuum wavenumber at the excitation frequency. A first node occurs at radius $r_1$ for the first zero of the Bessel function at $k_0 r_1 = 2.405$; at 100 MHz excitation frequency, $r_1 = 1.15$ m and so there is no node for the vacuum electric field within the reactor for the range of frequencies investigated here. The data in the figure are also compared with a numerical solution of Maxwell's equations which accounts for the boundary conditions imposed by the grounded sidewall. The deviation of the measurements from the theoretical curves is probably due to perturbations caused by the probe shaft and the window in the grounded sidewall.

The solution for the Gaussian-lens electrode predicts a uniform radial profile for the vertical electric field at the design frequency of the lens [8]. Convex (under-compensated) or concave (over-compensated) curves would be observed for frequencies above or below the design frequency respectively. The measured profiles correspond well with the theoretical curves, as expected for the vacuum case. The theory and the design and construction of the reactor with a Gaussian-lens electrode are therefore validated for the case of vacuum (no plasma). The next section investigates whether the uniform condition is maintained or perturbed by the presence of plasma in the parallel-sided gap between the plane electrode and the plane glass surface.

### B. Plasma uniformity measurements: parallel plate electrodes

Using parallel plate electrodes, radial profiles of the plasma optical emission intensity $I_{\mathrm{oes}}(r)$ and ion saturated current $I_{\mathrm{sat}}(r)$ were measured for three frequencies as shown in the left- and right-hand columns respectively of figure 3. Since the dependence on pressure was generally stronger than for the power, only the pressure range is shown with the RF power fixed at 200 W. All profiles are normalized to on-axis values. The general agreement between the $I_{\mathrm{oes}}(r)$ and $I_{\mathrm{sat}}(r)$ profiles lends confidence to the diagnostic methods. In presence of plasma between parallel plates, the vertical electric field Bessel function profile is modified to

$$E_z(r) = E_0 \mathrm{J}_0 \left[ k_{\mathrm{eff}} r \right] = E_0 \mathrm{J}_0 \left[ k_0 r \Re(\epsilon_{\mathrm{eff}}^{1/2}) \right] \tag{4}$$

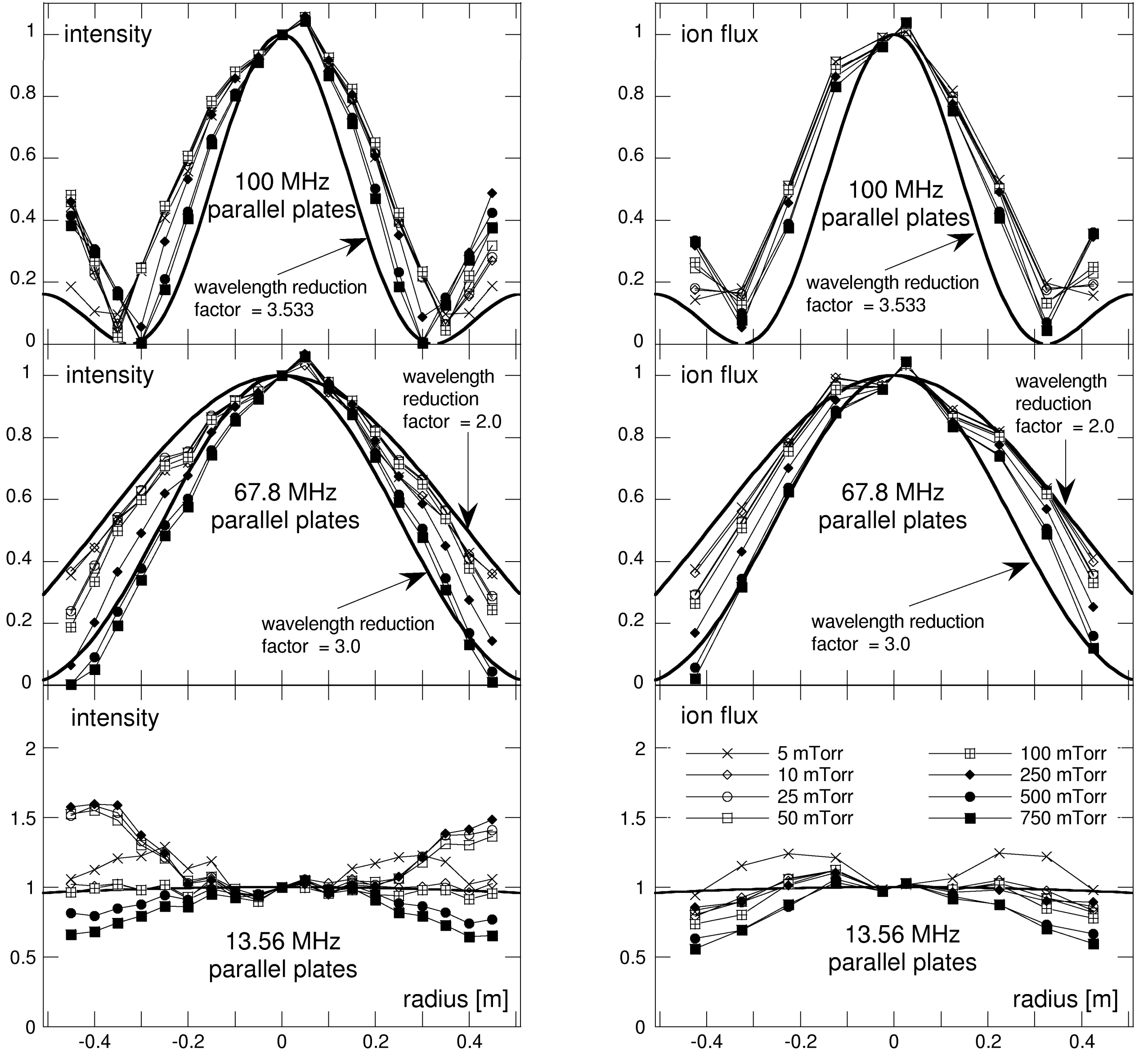


FIG. 3: Measured radial profiles of the plasma optical emission intensity $I_{\rm oes}(r)$ (left-hand column) and ion flux $I_{\rm sat}(r)$ (right-hand column) for three frequencies with parallel plate electrodes. The curves represent the square of the electric field described by a Bessel function and the corresponding wavelength reduction factor. All values are normalised to the values on axis. Error bars of $\pm 10\%$ are omitted for clarity. Argon pressure 5 to 750 mTorr and 200 W RF power.

where $k_{\rm eff} = k_0 \Re(\epsilon_{\rm eff}^{1/2})$ is the increased wavenumber of the wave propagating in the dielectric (with complex relative permittivity $\epsilon_{\rm eff}$) formed by the plasma-sheath combination (see Appendix A). $\Re(\epsilon_{\rm eff}^{1/2})$ is called the "wavelength reduction factor" in this paper. The factor $\Re(\epsilon_{\rm eff})$ can be considered as a sort of uniformity "worsening factor" as introduced by Schmitt

*et al* [12] which makes the uniformity of the electric field (and plasma) worse than for the vacuum case.

In order to compare the measured intensity profiles with theory for the case of parallel plates, we make an assumption that the optical emission intensity and ion flux are proportional to the square of the electric field which is approximately proportional to the local power dissipation. The optical emission profiles $I_{\text{oes}}(r)$ are therefore compared with

$$I_{\text{oes}}(r) = I_0 \left\{ \mathrm{J}_0 \left[ k_0 r \Re(\epsilon_{\text{eff}}^{1/2}) \right] \right\}^2 \tag{5}$$

in figure 3, and similarly for $I_{\text{sat}}(r)$. Because the plasma permittivity shortens the vacuum wavelength, the first node at 100 MHz now occurs within the reactor radius at $r_1 \approx 0.325$ m, where the plasma optical emission intensity and ion flux fall close to zero. This clearly demonstrates the strong non-uniformity when using VHF in large, parallel plate reactors. Since $k_0 r_1 \Re(\epsilon_{\text{eff}}^{1/2}) \approx 2.405$, we deduce a wavelength reduction factor $\Re(\epsilon_{\text{eff}}^{1/2}) \approx 3.5$ for the plasma at 100 MHz. Using the approximation $\Re(\epsilon_{\text{eff}}^{1/2}) \approx \sqrt{d_{\text{gap}}/2d_{\text{sh}}}$ in Appendix A, this corresponds to a sheath width of about 1.2 mm which is reasonable for this VHF plasma [16].

The wavelength reduction factor for the profiles at 67.8 MHz in figure 3 were in the range $2 < \Re(\epsilon_{\text{eff}}^{1/2}) < 3$, which corresponds to sheath widths from 3.75 mm to 1.66 mm using the model in Appendix A, as the pressure increased from 5 to 750 mTorr. The deduced sheath width is therefore observed to decrease with increasing pressure [17, 18] and frequency [16, 19], in general agreement with the literature. Note that the profiles at 67.8 and 100 MHz are very non-uniform, and dominated by the standing wave effect for the whole parameter range investigated. The profiles at 13.56 MHz, where standing wave effects are expected to be negligible for this reactor size, are approximately uniform except for edge effects, seen on many of the measured profiles, caused by fringing fields, hollow cathode ("focusing" of the electric field at the corners), and electrode area asymmetry [13].

For all the plasma parameters using parallel plates at the VHF frequencies 67.8 and 100 MHz, the principal non-uniformity in figure 3 is frequency-dependent and can be explained by the standing wave effect. Perret *et al* [20] found that edge or inductive effects [7] can strongly modify the standing wave power deposition profile at RF power densities higher than used in this paper.

The strong non-uniformity due to the standing wave effect would normally prohibit the

use of Very High Frequency for applications in large area reactors [4–8], thereby forgoing the advantages of VHF operation such as high deposition rate, and reduced sheath voltage and ion bombardment energy [1, 3, 12, 21]. The improved uniformity using VHF in a *small* highly-asymmetric reactor [3] was most likely due to an interplay with the dominant edge effects which coincidentally resulted in a better uniformity at 70 MHz than at 13.56 MHz.

### C. Plasma uniformity measurements: Gaussian-lens electrode

The profiles in figure 4 were obtained using the Gaussian-profile electrode filled with PTFE dielectric, designed for uniform vertical electric field at 69.0 MHz excitation frequency.

The measured profiles using this Gaussian-lens electrode at 67.8 MHz are more uniform than the corresponding profiles at 67.8 MHz with parallel plates in figure 3. Only edge effects remain to perturb the flat profile, which is similar to the situation for 13.56 MHz with parallel plates.

Figure 4 also shows the measured profiles when using 13.56 MHz. Using this frequency, which is below the lens design frequency, gives over-compensated, concave profiles. Conversely, excitation frequencies above the design frequency would give under-compensated, convex profiles.

Without the glass disc to confine the plasma between parallel planes, the observed plasma profiles are similar to the parallel-plate measurements, because the plasma "short-circuits" the electric field within the lens volume. The same is true if a plasma ignites underneath the glass when the power is too high and the volume is not evacuated - this was the case when using the lens at 100 MHz with no dielectric filling. This is why all the measurements in this work were made at 67.8 MHz, close to the design frequency of 69.0 MHz with the lens filled with PTFE, in order to avoid plasma in the lens gap below the glass.

To resolve the problem of non-uniformity when high frequency is combined with large area reactors, it is clear that two distinct issues must be addressed: the standing wave effect, and the edge effects. The standing wave effect is compensated by the Gaussian-lens electrode, whereas edge effects have always existed even at low frequency in parallel plate reactors. In practice, edge effects are pragmatically reduced by reactor design and process optimisization - a process window of plasma parameters is empirically determined where the

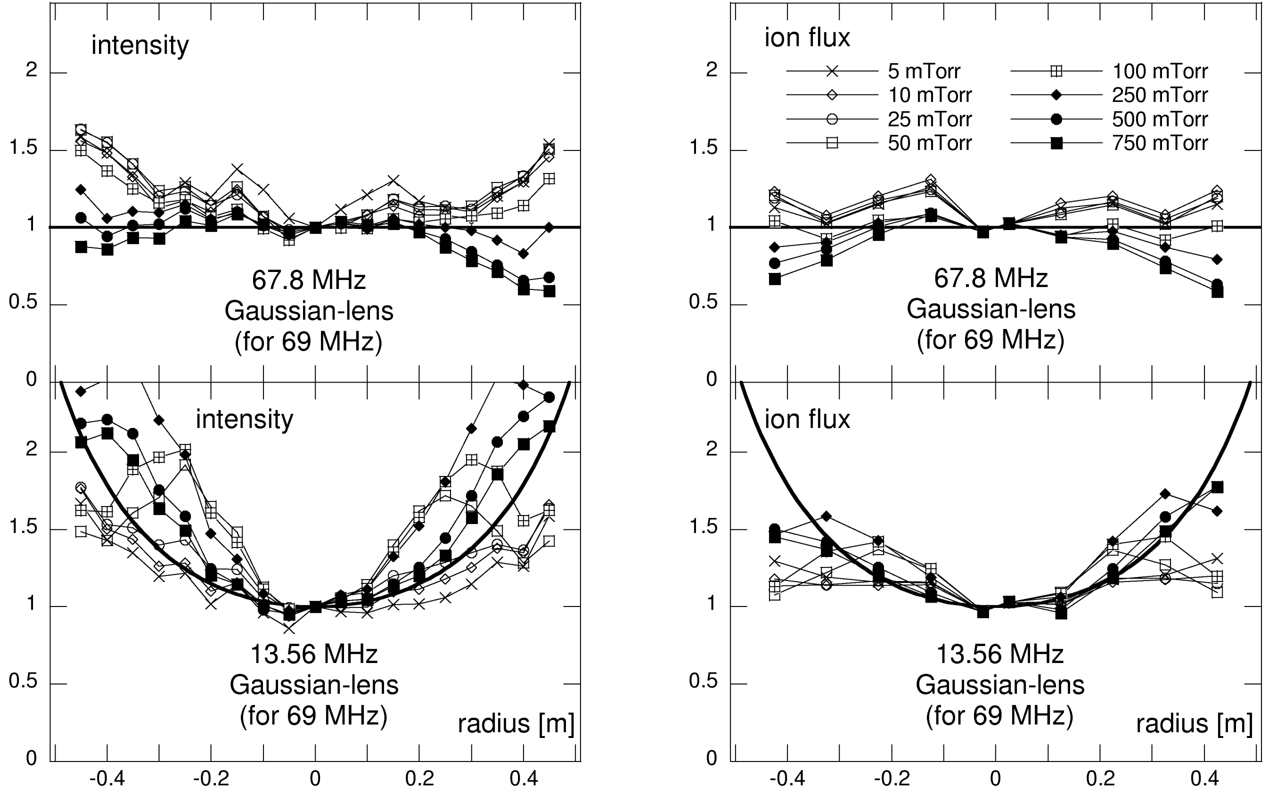


FIG. 4: Measured radial profiles of the plasma optical emission intensity $I_{\rm oes}(r)$ (left-hand column) and ion flux $I_{\rm sat}(r)$ (right-hand column) for the Gaussian-lens electrode filled with PTFE dielectric (design frequency 69.0 MHz). For the data at 13.56 MHz, the data are compared with the square of the electric field assuming capacitive division between the plasma sheath (assumed width 3.75 mm) and the electrode lens. All values are normalised to the values on axis. Error bars of $\pm 10\%$ are not shown for clarity. Argon pressure 5 to 750 mTorr and 200 W RF power.

necessary plasma properties are sufficiently uniform for the required application. In figure 5, for example, it is possible to select pressures and RF powers for good overall uniformity of the ion flux at 67.8 MHz using the Gaussian-lens electrode, whereas the profiles obtained with the parallel plate electrodes at this frequency remain dominated by the standing wave effect for all plasma parameters. This demonstrates the effectiveness of the Gaussian-lens electrode for compensating the standing wave effects for VHF plasmas in large area reactors.

Note that either the RF electrode or the ground electrode can be chosen to have the Gaussian-lens shape. Also, if a conducting substrate is to be used, it should be placed

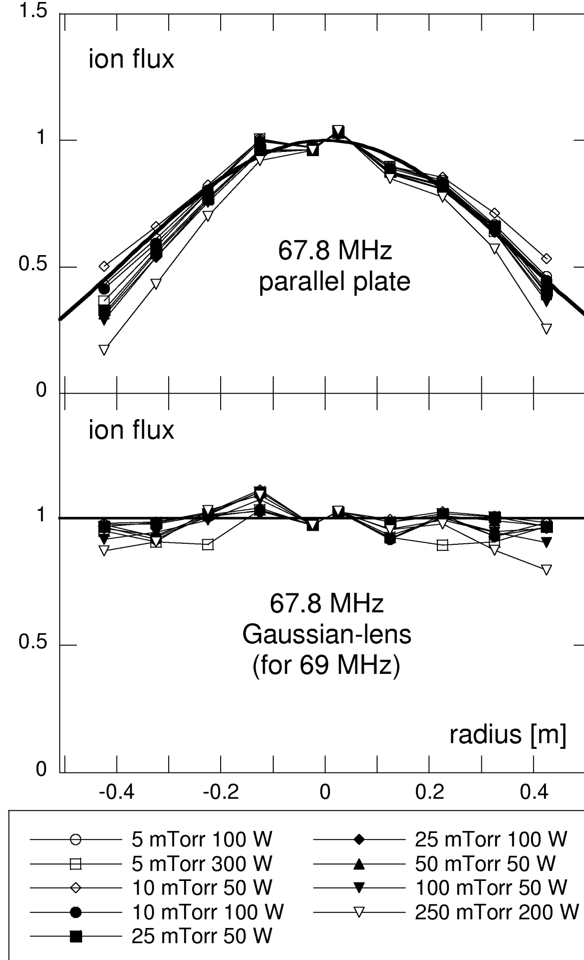


FIG. 5: Bottom: Measured radial profiles of the ion flux $I_{\text{sat}}(r)$ at 67.8 MHz for the Gaussian-lens electrode filled with PTFE dielectric (design frequency 69.0 MHz). Top: the same measurements but with parallel plate electrodes. Uniform profiles can be obtained using the lens electrode by suitable choice of pressure and RF power, whereas the profiles for parallel plate electrodes are strongly non-uniform and dominated by the standing-wave effect for all plasma parameters indicated. All values are normalised to the values on axis. Error bars of $\pm 10\%$ are not shown for clarity.

on the plane electrode, and not above the Gaussian-lens electrode, to avoid screening the electric field in the vicinity of the lens.

## IV. CONCLUSIONS

Plasma profile measurements of optical emission intensity and ion flux in a 1 m-diameter cylindrical reactor with Very High Frequency excitation (67.8 MHz in this paper, see figure

5) demonstrate the proof of principle of a Gaussian-lens electrode for removing the standing wave non-uniformity in large area reactors. The lens designed for a vacuum solution of Maxwell's equations at a given frequency remains valid in presence of plasma for a wide range of parameters. Very High Frequency excitation can therefore be combined with large area reactors without the non-uniformity problems of standing wave effects.

For all the plasma parameters investigated using parallel plates at 67.8 and 100 MHz the principal non-uniformity can be explained by the standing wave effect. In the absence of standing wave effects (low frequency with parallel plates or high frequency with lens electrode), any remaining non-uniformity is due to edge effects.

**Acknowledgments**

The authors thank Dr. Fiona Cook for careful reading of the manuscript. This work was funded by Swiss Federal Research Grant CTI 5602.1.

## APPENDIX A: EFFECTIVE DIELECTRIC CONSTANT FOR THE PARALLEL PLATE PLASMA-SHEATH SYSTEM

The plasma in the cylindrical axisymmetric parallel-plate reactor is generated by the RF excitation propagating inwards from the circumference [7, 8]. Since the spacing between the plates is much smaller than a half-wavelength, the frequencies used here are far below the cutoff of the first TM mode, and in vacuum, the excitation is a pure TEM mode with an azimuthal magnetic field and a vertical electric field. In presence of plasma, the magnetic field remains purely azimuthal, but due to the inhomogeneous dielectric, a radial electric field arises and the vacuum TEM mode is transformed into a quasi-TEM mode [22]. The distribution of the vertical electric field in this case is nearly the same as for electrostatic fields (quasi-static approximation) and the effective relative permittivity is given by [8, 12]

$$\epsilon_{\mathrm{eff}} = \left[ \frac{1}{d_{\mathrm{gap}}} \int_0^{d_{\mathrm{gap}}} \frac{dz}{\epsilon(z)} \right]^{-1} \tag{A1}$$

where $d_{\mathrm{gap}}$ is the electrode gap distance and $\epsilon(z)$ the $z$-dependent relative permittivity. For a simple model consisting of a series combination of a uniform plasma slab ($\epsilon(z) = \epsilon_{\mathrm{pl}}$) and vacuum sheaths ($\epsilon(z) = 1$), widths $d_{\mathrm{pl}}$ and $d_{\mathrm{sh}}$ respectively (so that $d_{\mathrm{gap}} = d_{\mathrm{pl}} + 2d_{\mathrm{sh}}$), the

effective relative permittivity is given by

$$\epsilon_{\rm eff} = \frac{d_{\rm gap}\epsilon_{\rm pl}}{2d_{\rm sh}\epsilon_{\rm pl} + d_{\rm pl}}. \tag{A2}$$

For plasma conditions where the magnitude of the plasma relative permittivity

$$\epsilon_{\rm pl} = 1 - \frac{\omega_{\rm pe}^2}{\omega(\omega - j\nu)} \tag{A3}$$

is much larger than 1 ($\omega_{\rm pe}$ is the electron plasma frequency and $\nu$ the electron-neutral collision frequency), the effective relative permittivity can be approximated by:

$$\epsilon_{\rm eff} \approx \frac{d_{\rm gap}}{2d_{\rm sh}}. \tag{A4}$$

This simply means that the effective capacitance of the electrode gap, $C_{\rm eff} = \epsilon_0\epsilon_{\rm eff}/d_{\rm gap}$, is approximately equal to the series capacitance of the two sheaths, $\epsilon_0/2d_{\rm sh}$, because the plasma impedance is negligible in comparison. This approximation is good for the pressures investigated in this work provided that the electron density is above $2 \cdot 10^9 {\rm cm}^{-3}$. The measured ion flux on axis was in the range 0.06 - 0.34 mA $\rm cm^{-2}$ corresponding to electron densities from about $2.8 \cdot 10^9 {\rm cm}^{-3}$ to $1.6 \cdot 10^{10} {\rm cm}^{-3}$ which is sufficient for validity of the approximation in Eq. A4 but not so high as to cause possible inductive skin effects [7, 20].

For the 30 mm electrode gap used in these experiments, the range of wavelength reduction factor deduced from the measurements in Section III B, namely $2 < \Re(\epsilon_{\rm eff}^{1/2}) \approx \sqrt{d_{\rm gap}/2d_{\rm sh}} < 3.5$, corresponds to physically-reasonable sheath widths of 3.75 mm $> d_{\rm sh} >$ 1.2 mm. This expression is the same as the approximation for the standing wave wavelength correction factor in Ref. [7].

The effect of the plasma permittivity for the Gaussian lens case will be treated in a future work.

[1] J. Kuske, U. Stephan, O. Steinke, and S. Rohlecke, Mat. Res. Soc. Symp. Proc **377**, 27 (1995).

[2] H. Curtins, N. Wyrsch, M. Favre, and A. V. Shah, Plasma Chem. Plasma Processing **7**, 267 (1987).

[3] A. A. Howling, J. L. Dorier, C. Hollenstein, U. Kroll, and F. Finger, J. Vac. Sci. Technol. A **10**, 1080 (1992).

[4] J. P. M. Schmitt, Thin Solid Films **174**, 193 (1989).

[5] J. P. M. Schmitt, Mat. Res. Soc. Symp. Proc **219**, 631 (1992).

[6] L. Sansonnens, A. Pletzer, D. Magni, A. A. Howling, C. Hollenstein, and J. P. M. Schmitt, Plasma Sources Sci. Technol. **6**, 170 (1997).

[7] M. A. Lieberman, J. P. Booth, P. Chabert, J. M. Rax, and M. M. Turner, Plasma Sources Sci. Technol. **11**, 283 (2002).

[8] L. Sansonnens and J. Schmitt, Appl. Phys. Lett. **82**, 182 (2003).

[9] L. Sansonnens, J. P. M. Schmitt, A. A. Howling, J. Ballutaud, H. Schmidt, and C. Hollenstein, in *Int. Colloq. Plasma Processes* (Antibes, France, 2003), p. 120.

[10] H. Meiling, W. G. J. H. M. van Sark, J. Bezemer, and W. F. van der Weg, J. Appl. Phys **80**, 3546 (1996).

[11] C. Hollenstein, A. A. Howling, C. Courteille, J.-L. Dorier, L. Sansonnens, D. Magni, and H. Müller, Mat. Res. Soc. Symp. Proc. **507**, 547 (1998).

[12] J. P. M. Schmitt, M. Elyaakoubi, and L. Sansonnens, Pl. Sources Sci. Technol. **11**, A206 (2002).

[13] J. Ballutaud, C. Hollenstein, A. A. Howling, L. Sansonnens, H. Schmidt, and J. P. M. Schmitt, in *Int. Symp. Pl. Chem. ISPC16* (Taormina, Italy, 2003).

[14] E. Pleuler, C. Wild, M. Füenr, and P. Koidl, Diamond and Related Materials **11**, 467 (2002).

[15] A. D. Colley, H. J. Baker, and D. R. Hall, Appl. Phys. Lett. **61**, 136 (1992).

[16] M. Fivaz, S. Brunner, W. Schwarzenbach, A. A. Howling, and C. Hollenstein, Pl. Sources Sci. Technol. **4**, 373 (1995).

[17] V. A. Godyak, R. Piejak, and B. M. Alexandrovich, IEEE Trans. Plasma Sci. **19**, 660 (1991).

[18] N. Mutsukura, K. Kobayashi, and Y. Machi, J. Appl. Phys. **68**, 2657 (1990).

[19] C. Beneking, J. Appl. Phys. **68**, 4461 (1990).

[20] A. Perret, P. Chabert, J.-P. Booth, J. Jolly, J. Guillon, and P. Auvray, Appl. Phys. Lett. **83**, 243 (2003).

[21] W. Schwarzenbach, A. A. Howling, M. Fivaz, S. Brunner, and C. Hollenstein, J. Vac. Sci. Technol. A **14**, 132 (1996).

[22] J. R. W. S. Ramo and T. V. Duzer, *Fields and Waves in Communication Electronics* (Wiley, 1994), chap. 8.